Comparison of UV-A photolytic and UV/TiO_2 photocatalytic effects on *Microcystis aeruginosa* PCC7813 and four microcystin analogues: a pilot scale study

Indira Menezes[a,b*], José Capelo-Neto[a], Carlos J. Pestana[b], Allan Clemente[a], Jianing Hui[c], John T. S. Irvine[c], H.Q. Nimal Gunaratne[d], Peter K.J. Robertson[d], Christine Edwards[b], Ross N. Gillanders[e], Graham A. Turnbull[e], Linda A. Lawton[b]

[a] Department of Hydraulic and Environmental Engineering, Federal University of Ceará, Fortaleza, Brazil

[b] School of Pharmacy and Life Sciences, Robert Gordon University, Aberdeen, United Kingdom

[c] School of Chemistry, University of St Andrews, St Andrews, United Kingdom

[d] School of Chemistry and Chemical Engineering, Queen's University, Belfast, United Kingdom

[e] Organic Semiconductor Centre, SUPA, School of Physics and Astronomy, University of St Andrews, St Andrews, United Kingdom

*Corresponding author: i.de-menezes-castro@rgu.ac.uk

Highlights

- UV-A photolysis was effective for elimination of cyanobacteria and toxins
- Complete inhibition of *M. aeruginosa* PCC7813 by UV-A photolysis
- 92% removal of four microcystins after UV-A photolysis (intra- and extracellular)
- TiO_2 photocatalysis was less effective in *M. aeruginosa* PCC7813 cell removal

Graphical abstract

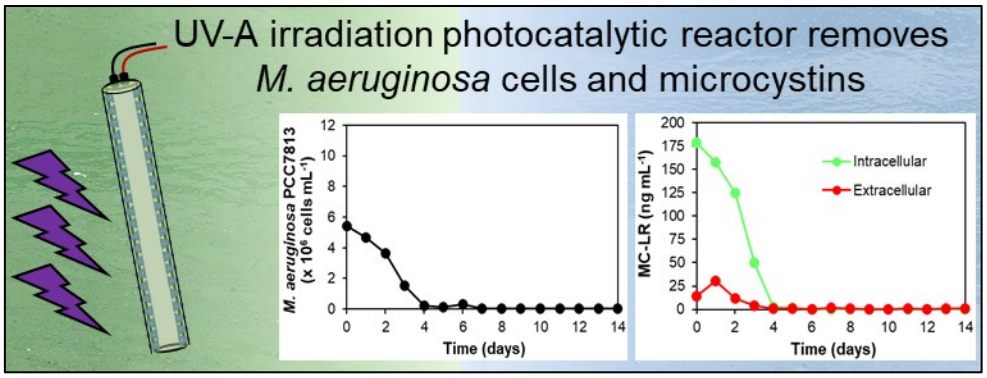

Abstract

To date, the high cost of supplying UV irradiation has prevented the widespread application of UV photolysis and titanium dioxide based photocatalysis in removing undesirable organics in the water treatment sector. To overcome this problem, the use of UV-LEDs (365 nm) for photolysis and heterogeneous photocatalysis applying TiO_2 coated glass beads under UV-LED illumination (365 nm) in a pilot scale reactor for the elimination of *Microcystis aeruginosa* PCC7813 and four microcystin analogues (MC-LR, -LY, -LW, -LF) with a view to deployment in drinking water reservoirs was investigated. UV-A (365 nm) photolysis was shown to be more effective than the UV/TiO_2 photocatalytic system for the removal of *Microcystis aeruginosa* cells and microcystins. During photolysis, cell density significantly decreased over 5 days from an initial concentration of 5.8 x 10^6 cells mL^{-1} until few cells were left. Both intra- and extracellular microcystin concentrations were significantly reduced by 100 and 92%, respectively, by day 5 of the UV treatment for all microcystin analogues. During UV/TiO_2 treatment, there was great variability between replicates, making prediction of the effect on cyanobacterial cell and toxin behavior difficult.

Keywords: blue-green algae; cyanotoxins; water treatment; titanium dioxide, cyanobacteria

1 Introduction

Cyanobacterial blooms in freshwater reservoirs represent a threat to human and animal health because of the potential release of a wide variety of harmful metabolites, known collectively as cyanotoxins (Carmichael *et al*., 2001; Falconer *et al*., 1983; Jochimsen *et al*., 1998). Microcystins (MCs) are one of the most commonly reported cyanotoxins with over 247 analogues to date (Spoof and Catherine, 2017). Conventional water treatment (i.e., coagulation, flocculation, sedimentation or flotation and filtration) is used worldwide for treatment of water contaminated with cyanobateria, however, these processes can promote cell rupture and consequently cyanotoxin release into the environment (Chang *et al*., 2018; Pestana *et al*., 2019). Further, conventional treatment methods are designed for the removal of suspended or colloidal particles and are not fit to remove dissolved contaminants including dissolved cyanotoxins (Chae *et al*., 2019; Vilela *et al*., 2012). In order to mitigate the effect of dissolved cyanobacterial toxins entering water treatment plants, advanced oxidation processes (AOPs) such as photocatalysis and photolysis can be used for the control of cyanobacterial cells and toxic metabolites within reservoirs (Fan *et al*., 2019; Matthijs *et al*., 2012; Ou *et al*., 2011a).

UV photolysis is an AOP that has been widely applied for the inactivation of pathogenic microbes in water treatment and other applications, and can be used as a strategy for removing cyanobacteria and their toxins. A number of studies have evaluated the effects of mainly UV-C (usually 254 nm) and UV-B (usually 312 nm) on microcystin degradation and *Microcystis aeruginosa* removal (Liu *et al*., 2010; Moon *et al*., 2017; Tao *et al*., 2018). This, however, is the first time that the degradation of *M. aeruginosa* PCC7813 and four microcystin analogues (MC-LR, MC-LW, MC-LY, MC-LF) under UV-A (365 nm) irradiation was investigated.

UV-irradiation-driven titanium dioxide (TiO_2) photocatalysis is another AOP that can be used to control cyanobacteria and their toxins. TiO_2 activation needs to occur under UV light irradiation ($\lambda < 387$ nm) (Chang *et al*., 2018; Hu *et al*., 2017; Zhao *et al*., 2014) due to its wide band gap (3.2 eV and 3.0 eV for the anatase and rutile forms of TiO_2

respectively) (Chen *et al*., 2015; Hu *et al*., 2017; Pinho *et al*., 2015b), which limits its application in drinking water treatment (Jin *et al*., 2019). UV light is, however, attenuated by water and hence the need for UV irradiation (below 387 nm) is a hurdle in the practical application of photolysis and photocatalysis for water treatment (Chae *et al*., 2019). To overcome this, and to make the systems practical for application in reservoirs used for drinking water, the system investigated here employs UV (365 nm) light emitting diodes (LEDs), which are low-cost (ca. USD 0.78 per LED), long life (approximately 100,000 working hours; Heering, 2004) and capable of activating TiO_2. In the current study, UV-LED-driven photolysis and TiO_2 photocatalysis were evaluated over 14 days for the elimination of *M. aeruginosa* PCC7813 as well as for the destruction of four microcystin analogues (MC-LR, MC-LW, MC-LY, MC-LF).

2 Methods

2.1 Reagents

The chemicals for artificial fresh water (AFW) and BG-11 culture medium (Stanier *et al*., 1971) preparation were of reagent grade (Fisher Scientific, UK). AFW was prepared according to Akkanen and Kukkonen (2003) by dissolving $CaCl_2$ (11.8 mg L^{-1}), $MgSO_4$ (4.9 mg L^{-1}), $NaHCO_3$ (2.6 mg L^{-1}) and KCl (0.2 mg L^{-1}) in ultrapure water. For AFW, pH was adjusted to 7 with 1 M hydrochloric acid or 1 M sodium hydroxide if required. Acetonitrile, methanol, and trifluoroacetic acid used for high performance liquid chromatography analysis of microcystins were of HPLC grade (Fisher Scientific, UK). Diuron (3-(3,4-dichlorophenyl)-1,1-dimethylurea) (Sigma-Aldrich, UK) was used for photosynthetic activity assays. Isoton II Diluent obtained from Beckman Coulter (USA) was used for cyanobacterial cell density determination. All solutions were prepared using ultrapure water (18.2 MΩ) provided by an ELGA PURELAB system (Veolia, UK).

2.2 Cyanobacterial cultivation

The cyanobacterium *M. aeruginosa* PCC7813 (Pasteur Culture Collection) was grown

in BG-11 medium at 21±1 °C with constant cool white fluorescent illumination with an average light intensity of 30 µmol photons m^{-2} s^{-1} and constant sparging with sterile air. This strain does not have gas vesicles and produces four main microcystin analogues (MC-LR, MC-LY, MC-LW and MC-LF).

2.3 Reactor design for *M. aeruginosa* PCC7813 and microcystins treatment

A cell suspension of a 27 days-old culture of *M. aeruginosa* PCC7813 (5 x 10^6 cells mL^{-1}) in AFW was prepared and sampled prior to addition to the reactors (C_0). The reactors (1000 x 90 mm) were made of a stainless-steel mesh with an aperture of 1.2 x 1.2 mm and 0.4 mm wire strength. Each reactor was placed inside an acrylic cylinder (1100 x 95 mm) that was filled with 6.5 liters of *M. aeruginosa* suspension. The acrylic cylinders were sparged from the bases through a multi-porous air-stone with sterile air with the aid of a pump for continuous gentle air flow (1 L min^{-1} per reactor; Figure S1). The top of the acrylic cylinders was covered with a foam bung to avoid external contamination and to allow air exchanges. The overhead ambient light was of low intensity (2.5 µmol photons m^{-2} s^{-1}). Triplicate reactors were prepared for each of the tested systems (UV-only, TiO_2-only and UV/TiO_2).

One set of three reactors for the UV-A treatment (photolysis) was prepared (Figure S1A) which consisted of reactors with 5 UV-LED strips (1 meter), each with 120 individual UV-LEDs (λ=365 nm and light intensity of 5 W m^{-2}), attached to the external surface of the acrylic cylinders and 6.5 L of the cyanobacterial cell suspension added. In the UV-A treatment, empty tetrahedral stainless-steel wire mesh pods (aperture 1.2 x 1.2 mm, wire strength 0.4 mm, Figure S2) were placed inside the reactors without TiO_2 coated glass beads to allow observation of the effects of only UV-A light on *M. aeruginosa* PCC7813 and its four microcystin analogues. To determine if the TiO_2 coated beads have an effect on the cyanobacterial cells and toxins in the absence of UV light, a second set of triplicate reactors was prepared (Figure S1B), consisting of 6.5 L of the *M. aeruginosa* PCC7813 suspension and TiO_2 coated glass beads (3.2 g)

corresponding to 0.1% (w/v) TiO_2 inside tetrahedral stainless-steel pods (Figure S2). The TiO_2 coated beads were manufactured from recycled glass that were prepared as per Pestana *et al*. (2020) and Hui *et al*. (2021) containing approximately 12% (w/w) TiO_2. In the TiO_2-only samples, no UV illumination was used. Finally, a third set of reactors to test the efficacy of TiO_2 photocatalysis was prepared. The UV/TiO_2 treatment consisted of reactors with TiO_2 coated glass beads inside of the stainless-steel pods (Figure S2), 5 UV-LED strips and 6.5 liters of *M. aeruginosa* cell suspension (Figure S1C). All reactors were maintained in the presence low light intensity (2.5 µmol photons m^{-2} s^{-1}) from overhead lighting since photosynthetic organisms like cyanobacteria require light to survive.

Samples were collected and temperature measured (supplementary material S2) at the same time every day over 14 days. A total of 4 mL was removed at each sampling point, of which 1.5 mL was used for cell enumeration, 1.5 mL was used for intra/extracellular microcystin analysis and 1 mL was used for photosynthetic activity measurements. All aliquots were used immediately except for the aliquots for toxin determination, which were centrifuged for 10 minutes at 13000 G and the supernatant and cell pellets were stored separately at -20 °C until further processing and analysis.

2.4 *M. aeruginosa* PCC7813 regrowth experiment

To assess the regrowth of *M. aeruginosa* PCC7813 after 14 days treatment, samples (50 mL) were removed from each reactor and mixed with an equal volume of BG-11 medium. Aliquots of this mixture (3 mL) were transferred to 28 sterile glass vials (4 mL volume) to allow for sacrificial sampling over seven days with four replicate samples. Samples for each sampling point (i.e., 4 vials) were incubated in a sterile glass beaker (150 mL), covered with a sterile petri dish lid (Figure S3). Immediately, one set of samples was removed and cell density was analyzed (C_0 sample), the remaining beakers were incubated at 21±1 °C on a 12/12 hours light/dark cycle illuminated by cool white fluorescent lights with an average light intensity of 10.5 µmol photons m^{-2} s^{-1}

without agitation for the following 6 days and sampled at the same time every day.

2.5 Analysis

2.5.1 *M. aeruginosa* PCC7813 cell density determination

M. aeruginosa PCC7813 cell density was measured with a Multisizer 3 (Beckman Coulter, USA). A 50 µm aperture tube was used to detect particle sizes from 1 to 7 µm for both reactor treatments and regrowth experiments. Samples were diluted 200 to 1500-fold in Isoton II Diluent (Beckman Coulter, USA), depending on the sample cell density.

2.5.2 *M. aeruginosa* PCC7813 photosynthetic activity evaluation

A Mini-PAM system (Walz, Germany) was used for cyanobacterial photosynthetic activity analysis according to Menezes *et al*. (2020). In short, the minimal fluorescence F_0 was measured by adding 400 µL of sample into a cuvette under agitation followed by diuron (0.5 M) addition (20 µL) and the true maximal fluorescence measurement (F_M') by a saturating pulse under actinic light. The cyanobacterial photosynthetic activity can be determined by the maximal values of quantum yield of photosystem (PS) II calculated by F_V/F_M', where F_V is the difference between F_M' and F_0 (Stirbet *et al*., 2018).

2.5.3 Intra- and extracellular microcystin determination by high-performance liquid chromatography (HPLC)

After sampling, the liquid and solid portions of the sample were separated in a centrifuge for 10 minutes at 13000 G. The supernatant, representing the extracellular toxin component, was evaporated to dryness in an EZ-II evaporator (Genevac, UK). Dried samples were resuspended in 80% aqueous methanol (150 µL) and stored at -20 °C until analysis. Cell pellets, representing the intracellular toxin component, were resuspended in 80% aqueous methanol (150 µL), agitated in a dispersive extractor for

5 minutes at 2500 rpm and centrifuged for 10 minutes at 13000 G to remove cell debris. The resultant supernatant, representing the liberated intracellular content was stored at -20 °C until analysis. The concentrations of four microcystin analogues (MC-LR, MC-LY, MC-LW and MC-LF) were quantified by HPLC (Table 1).

Table 1 – Analytical conditions of HPLC for intra- and extracellular microcystins determination.

Parameters	Conditions					
HPLC	2965 separation module and a 2996 photodiode array (PDA) detector (Waters, United States)					
Column	Symmetry C18 column, 2.1 mm x 150 mm, 5 µm particle size (Waters, United States)					
Mobile phase	A: 0.05% trifluoroacetic acid in ultrapure water (18.2 MΩ) B: 0.05% trifluoroacetic acid in acetonitrile					
Gradient	Time (min)	0	25	26	29	35
	Solvent A (%)	80	30	0	80	80
Flow rate	0.3 mL min^{-1}					
Injection volume	35 µL					
Column temperature	40 °C					
PDA scan range	200-400 nm					

All chromatograms were extracted at 238 nm and quantified using standards (as per Enzo Life Sciences) for calibration between 0.001 and 5 µg mL^{-1} in the Empower software. The limit of quantification was 0.01 µg mL^{-1} for MC-LF and 0.005 µg mL^{-1} for the other microcystin analogues.

2.7 Statistical data analyses

All statistical analyses were performed using RStudio with a significance level of 5%. In order to verify if the TiO_2-only samples, UV and UV/TiO_2 treatments influenced cell numbers or toxin removal it is necessary to identify a significant reduction of cell density during treatment and intra- and extracellular microcystin concentration (dependent variables) over 14 days (independent variable). The results were pre-analyzed using different statistical models, i.e., linear, piecewise, linear-plato,

exponential and logarithmic regression. The models were selected and adjusted using the linear or piecewise regression techniques using the mean of triplicates from each treatment group. The linear or piecewise regression techniques were selected because they were the models that presented the best fit with the data. The mean was selected to create each model because the mean values presented normal distribution according to Shapiro-Wilk Normality Test (data not shown). The linear regression consists in a linear relation between dependent (cell density and microcystins concentration) and independent (time) variables. The piecewise regression consists in multiple linear models to the data for different ranges of the independent variable, which means that the tendency/inclination of the curve of the dependent variable will change over the independent variable. A detailed description of the data analysis and the model selection can be found in the supplementary material (S4).

3 Results and Discussion

3.1 Treatment effects on *Microcystis aeruginosa* PCC7813 cell density and photosynthetic activity

The removal of *M. aeruginosa* PCC7813 in a photocatalytic and a photolytic reactor using UV-LEDs and TiO_2 coated beads was investigated. The effect of the UV-A treatment presented a piecewise regression tendency (Figure S4) with a cell density decrease from 5.4×10^6 cells mL^{-1} over 5 days until there were only 1.8×10^4 cells mL^{-1} left (significant tendency rate of 1.12×10^6 cells mL^{-1} day^{-1} until 5 days, $p<0.01$; Figure 1A).

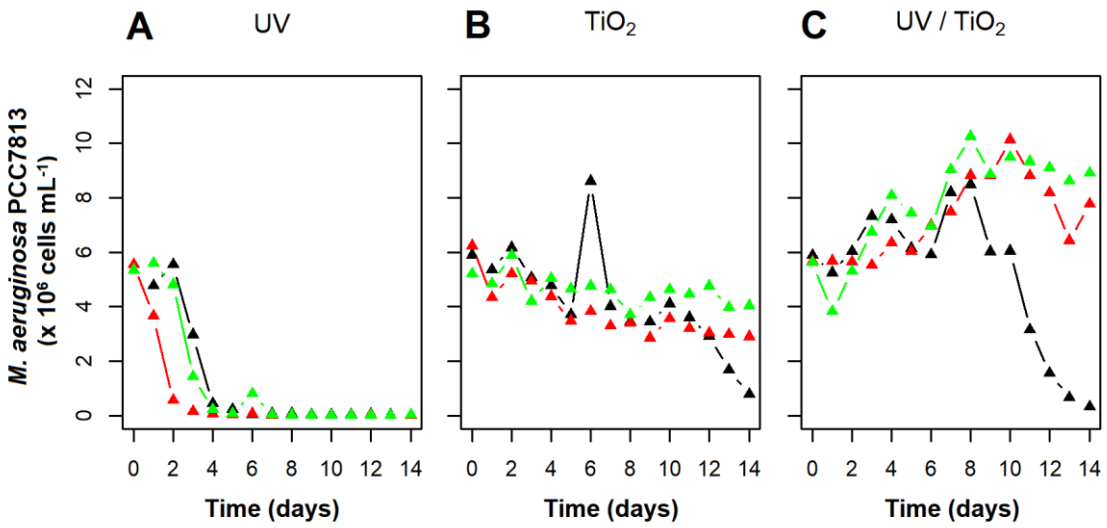

Figure 1 – Effects of (A) UV-LED irradiation (365 nm), (B) TiO_2 coated glass beads under ambient light (2.5 µmol photons m^{-2} s^{-1}) and (C) photocatalytic treatment on *Microcystis aeruginosa* PCC7813 cell density using TiO_2 coated glass beads under UV-LED illumination (365 nm) over 14 days, sparged with sterile air. Data points represent individual replicates for each treatment.

Biological replicates can commonly present different behaviors even when exposed to very similar conditions. *M. aeruginosa* PCC7813 cell numbers showed slightly different trends during TiO_2-only treatment with variability increasing as the investigation progressed, particularly after day 10. The outlier observed on day 6 probably occurred due to lack of mixing during cell counting, since samples were consistent until day 10. *M. aeruginosa* PCC7813 cell numbers decreased on average from 5.8 x 10^6 to 2.6 x 10^6 cells mL^{-1} with a significant rate of 0.19 x 10^6 cells mL^{-1} day^{-1} (p<0.01) over 14 days (Figure 1B) represented by linear regression (Figure S5). The variability that increased over time might have occurred due to adsorption of cells onto the surface of the TiO_2 layer on the beads and to adhesion of cells onto the inside walls of the reactor.

A reduction in cell numbers was expected to be observed in the UV/TiO_2 treatment on the *M. aeruginosa* PCC7813 cell density based on previous bench-scale studies (Pestana *et al.*, 2020; Chang *et al.*, 2018; Song *et al.*, 2018; Wang *et al.*, 2018, 2017; Pinho *et al.*, 2012). However, the *M. aeruginosa* cell density could best be represented by a piecewise regression tendency (Figure S6) and significantly rose in the UV/TiO_2

250 treatment over the first eight days with a tendency rate of 0.46 x 10^6 cells mL^{-1} day^{-1}
251 (p<0.01), and then decreased after day 8 with a tendency rate of 1 x 10^6 cells mL^{-1} day^{-1}
252 (p<0.01; Figure 1C). One possible explanation for this observation is that the TiO_2
253 coated glass beads have converted some of the incoming UV irradiation into visible
254 light through fluorescence from the semiconductor material (Li *et al*., 2016) in sufficient
255 quantities to support modest growth, despite the fact that ambient overhead light was
256 of low intensity (2.5 µmol photons m^{-2} s^{-1}) and nominally insufficient for significant cell
257 growth evidenced by no growth observed in the treatments without LEDs (Figure 1B).
258 Photoluminescence measurements of the TiO_2 coated glass beads show that the
259 beads generate additional visible light, albeit with low efficiency of 7%. The spectrum
260 was generated at a wavelength of around 430 nm, presenting an overlap with the blue
261 absorption peak of chlorophyll *a*, which can be used by cyanobacteria since chlorophyll
262 *a* has a significant absorbance at this same wavelength and might have contributed to
263 growth of the cyanobacteria (supplementary material S5). It is possible that at the same
264 time cells were receiving sufficient light to grow, during UV/TiO_2 treatment, cells were
265 being damaged and growth was inhibited. Mathew *et al*. (2012) also observed
266 emission of new wavelengths in the range of visible light (387, 421, 485, 530 and 574
267 nm) from TiO_2 colloidal nanoparticles after the excitation wavelength of 274 nm. The
268 sample behavior after day 8 is not a true reflection of the individual replicates. After 8
269 days, the replicate treatments diverged with one of the replicates (Figure 1C: black)
270 declining rapidly (cell density decreased from 5.8 x 10^6 to 3.1 x 10^5 cells mL^{-1}), while
271 the two other replicates (Figure 1C: red and green) grew, with a cell density increasing
272 from 5.6 x 10^6 to 7.7 x 10^6 cells mL^{-1} for one of these replicates (red) and from 5.6 x 10^6
273 to 8.9 x 10^6 cells mL^{-1} in the other (green).
274 In order for the UV illumination to target a specific organism or to activate a catalyst, it
275 must be able to first transmit through the water (Summerfelt, 2003). The lack of cell
276 removal by photocatalysis in two out of three samples during the UV/TiO_2 treatment
277 could be explained by the air flow within the reactor design. In the UV/TiO_2

278 photocatalytic treatment, coated beads inside of the pods may have dispersed the
279 rising air flow into smaller air bubbles, thus attenuating the light to the point where an
280 insufficient number of photons reached the TiO_2 to produce hydroxyl radicals that would
281 be responsible for *M. aeruginosa* PCC7813 removal. The sparging pattern in the
282 reactor where photocatalytic removal of *M. aeruginosa* PCC7813 was observed may
283 have been such that permitted better light penetration, allowing the activation of TiO_2
284 coated beads by UV illumination and subsequent sufficient hydroxyl radical production.
285 Direct photolysis and the indirect oxidation by extracellular reactive oxygen species
286 (ROS) initially cause cellular stress and then damage to the cell membrane, without
287 promoting the complete destruction of the cell (Ou *et al*. 2011a, 2011b). Photosynthetic
288 activity as expressed as the F_V/F_M' ratio is a rapid method that can represent the level
289 of stress and/or damage in cyanobacterial cells (Menezes *et al*., 2020; Stirbet *et al*.,
290 2018; Yang *et al*., 2013). Cyanobacterial stress causes a decline in the F_V/F_M' ratio,
291 which means that the lower the F_V/F_M' ratio (photosynthetic activity) the more damage
292 or stress there is to the cyanobacteria. During the UV treatment, cyanobacterial cells
293 suffered inhibition of photosynthetic activity especially at the beginning of the
294 experiment from days 1 to 4 (Figure 2A). The photosynthetic activity decrease
295 observed during photolysis corresponds to the decrease in the cell number observed
296 until day 3 (Figure 1A). As previously reported by Menezes *et al*. (2020), photosynthetic
297 activity measurements showed a faster response to cell damage than cell density
298 measurements, indicating that cell stress occurred as early as 24 hours before cell
299 density changes could be observed by cell density measurements. The cell stress
300 results from day 3 are most likely due to the very low cell density observed from that
301 point in time (5×10^5 cells mL^{-1}), which were lower than the minimum concentration of
302 cells required for cell stress determination. For the TiO_2-only treatment photosynthetic
303 activity remained consistent for the first 6 days (Figure 2B), remaining at the same level
304 for two out of the three replicates until the end of 14 days (Figure 2B: red and green).
305 These results support the hypothesis from cell density observations (Figure 1B) that

cells were not inhibited or damaged but were removed from suspension and thus influencing the cell enumeration. Before carrying out the study, UV/TiO_2 treatment was expected to be the most effective treatment through damage to the photosynthetic system of *M. aeruginosa* PCC7813. However, relatively little effect was observed in the UV/TiO_2 treatment over the first 8 days with only one of the replicates showing a decline in photosynthetic activity from day 7 onwards (Figure 2C: black) which also corresponds to the cell density decrease in that replicate. (Figure 1C: black).

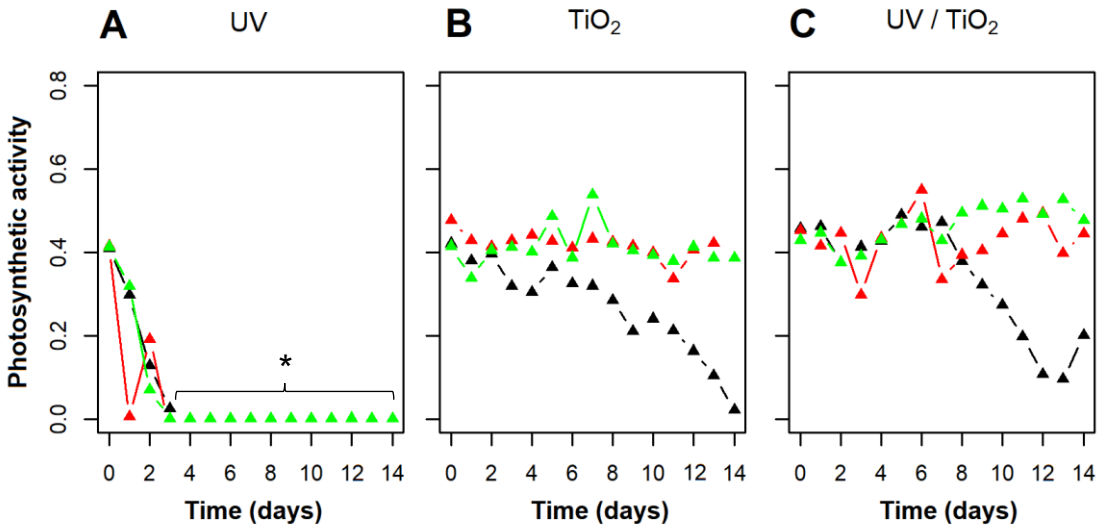

Figure 2 – Effects of (A) UV-LED irradiation (365 nm), (B) TiO_2 coated glass beads under ambient light (2.5 µmol photons m^{-2} s^{-1}) and (C) photocatalytic treatment on *Microcystis aeruginosa* PCC7813 photosynthetic activity using TiO_2 coated glass beads under UV-LED illumination (365 nm) over 14 days under sparging with sterile air. Data points represent individual replicates from each treatment. *Data points below the limit of quantification as too few cells remained for reliable quantification.

An initial decrease of *M. aeruginosa* PCC7813 cell density at the beginning of the experiment was expected which was what had been observed previously in other studies that evaluated *M. aeruginosa* cell density after TiO_2 photocatalytic treatment (Pestana *et al*., 2020; Chang *et al*., 2018; Song *et al*., 2018; Wang *et al*., 2018, 2017; Pinho *et al*., 2012). In particular, the study of Pestana *et al*. (2020), was a similar experimental design albeit in a smaller bench scale (30 mL of cell suspension and 700 mg of coated beads, equivalent to 0.2% (w/v) TiO_2). The differences in results between

323 the two studies could be due to the light attenuation of the bubbles being dispersed by
324 the beads.
325 In the current study, photolysis by UV illumination (365 nm) was observed to be the
326 most effective treatment for *M. aeruginosa* PCC7813 cell destruction. The reduction in
327 the *M. aeruginosa* PCC7813 cell density (Figure 1A) might be explained by the fact that
328 cyanobacteria do not produce sufficient ROS-scavenging enzymes (e.g., ROS
329 produced by UV treatment; Sinha *et al*., 2018). ROS oxidize lipids and proteins inside
330 the cyanobacterial cells, resulting in cell wall damage, followed by inactivation of
331 enzymes and ultimately cell death (Sinha *et al*., 2018). Furthermore, the effect of the
332 UV treatment on *M. aeruginosa* PCC7813 cells might have been caused by indirect
333 oxidation due to intracellular ROS (Ou *et al*. 2011a, 2011b). Intracellular ROS
334 generation may have been enhanced by the presence of intracellular phycocyanin
335 which is a natural cyanobacterial pigment (Robertson *et al*., 1999). Robertson *et al*.
336 (1999) suggested that cell destruction can occur from the inside-out rather than the
337 outside-in due to the production of both singlet oxygen and hydroperoxide radical
338 facilitated by the intracellular phycocyanin upon UV-irradiation. After this, the
339 intracellular ROS effects on cells were enhanced by phycocyanin, causing complete
340 degradation of cells. Under UV illumination alone, phycocyanin can contribute to the
341 degradation of cells by two mechanisms: firstly, during the electron transfer process
342 (Equation 1), the photoexcited phycocyanin transfers an electron to oxygen, producing
343 the superoxide radical that then becomes a hydroperoxide radical by protonation.
344 Secondly, during the energy transfer process (Equation 2), phycocyanin and oxygen
345 interact to produce singlet oxygen (Robertson *et al*., 1999) with both ROS attacking the
346 cell structures from within.

347 $$\mathbf{Phycocyanin} + \boldsymbol{h\nu} + \mathbf{O_2} \rightarrow \mathbf{Phycocyanin} + \bullet \mathbf{O_2^-}$$

348 $$\bullet \mathbf{O_2^-} + \mathbf{H^+} \rightarrow \bullet \mathbf{OOH} \qquad \text{(Equation 1)}$$

349 $$\mathbf{Phycocyanin} + \boldsymbol{h\nu} + \mathbf{O_2} \rightarrow \mathbf{Phycocyanin} + {}^1\mathrm{O}_2 \qquad \text{(Equation 2)}$$

350 Furthermore, cyanobacteria release oxygen during photosynthesis which can interact

with UV light and other organic compounds to produce ROS (Pattanaik *et al*., 2007). The ROS produced by UV-A illumination in the present study might also be responsible for damaging *M. aeruginosa* PCC7813 cells.

UV-C (254 nm) has been widely applied as a germicide for the inactivation of bacteria and viruses by denaturing the DNA of microorganisms and causing death or function loss (Boyd *et al*., 2020; Summerfelt, 2003). However, it is likely that the UV-A illumination (365 nm) used in the present study was able to destroy *M. aeruginosa* PCC7813 cells due to the generation of ROS and the presence of phycocyanin inside the cyanobacterial cells. Therefore, unlike UV-C illumination, UV-A illumination might be specific to cyanobacterial control and it may not affect other phytoplankton such as diatoms or green algae, although this requires further confirmation. The specificity of the effects of the UV-A photolysis on cyanobacteria would impact the phytoplankton community in natural waterbodies less than the application of UV-B/UV-C photolysis. At the same time, having the additional advantage of presenting with lower capital cost. Previous studies have investigated the application of other treatments (e.g., hydrogen peroxide oxidation) and observed that some treatment were selective for cyanobacterial species due to their biochemistry (Drábková et al., 2007a; Drábková et al., 2007b; Matthijs et al., 2012).Ou *et al*. (2011a, 2011b) pointed out that the UV-C-induced damage occurs via either direct photolysis or indirect oxidation by intra- and/or extracellular ROS. UV irradiation causes damage to the photosynthesis system, including PS I, PS II and phycobilisome which interrupts the electron transport chain and retards the critical reactions during photosynthesis, followed by the decomposition of cytoplasmic inclusions and finally cell destruction with release of intracellular organic matter. The same mechanisms might have occurred during the present UV-A photolysis where the photosynthetic system of *M. aeruginosa* PCC7813 was affected (Figure 2A) and cellular destruction occurred due to intracellular ROS (Figure 1A). Yang *et al*. (2015) evaluated the effects of high-energy UV-B illumination (280–320 nm) on a toxic (FACHB 915) and a non-toxic (FACHB 469) strain of *M. aeruginosa* photosynthetic

activity. The UV-B irradiation resulted in an inhibition of the photosynthetic activity of both toxic and non-toxic strains over 3 days of exposure due to damage to photosystem II (Yang *et al*., 2015). However, both *M. aeruginosa* strains used by Yang *et al*. (2015) showed signs of photosynthetic activity recovery at the end of the experiment.

3.2 Intra- and extracellular microcystin removal

The intracellular microcystin concentration for all analogues diminished significantly in a piecewise regression tendency (Figure S7 – S10) over the first 5 days of the UV treatment (Figure 3A) with the complete removal of all microcystin analogues by this time (approximate rate of 40, 22, 15 and 2.6 ng mL^{-1} day^{-1} of intracellular MC-LR, MC-LF, MC-LW and MC-LY, respectively, $p<0.01$ for all samples). The decrease of all four analogues of intracellular microcystins during UV treatment (Figure 3A) corresponds to the reduction of *M. aeruginosa* cell density and subsequent microcystins leak (Figure 1A). For the TiO_2-only samples (Figure 3B), the mean values suggest removal of 20, 43, 42 and 42% of intracellular MC-LR, MC-LF, MC-LW and MC-LY, respectively, or a significant decrease in a linear regression rate (Figure S11 – S14) of 3.7, 2.8, 2.9 and 0.3 ng mL^{-1} day^{-1} (for all samples $p<0.05$) over 14 days. Samples remained consistent over the first 11 days, however, it was possible to observe divergence in the results in the later stages. During UV/TiO_2 treatment, intracellular microcystins samples presented high variability over 14 days (Figure 3C) and while one replicate (Figure 3C: black) showed complete removal of all microcystins at the end of the experiment, another replicate (Figure 3C: green) demonstrated microcystins concentration of 157, 74, 59 and 11 ng mL^{-1} for MC-LR, MC-LF, MC-LW and MC-LY respectively. It is noteworthy that across all the treatments all microcystin analogues behaved in a similar manner (Figure 3), for example, one replicate during the UV treatment (Figure 3A: red) all analogues decreased on day 2, followed by the other two replicates on day 4 (Figure 3A: green and black). Variability in the toxin concentrations observed in Figure

3C is a further indication that both cell lysis due to UV/TiO_2 and cell growth due to the production of visible light are acting in the system.

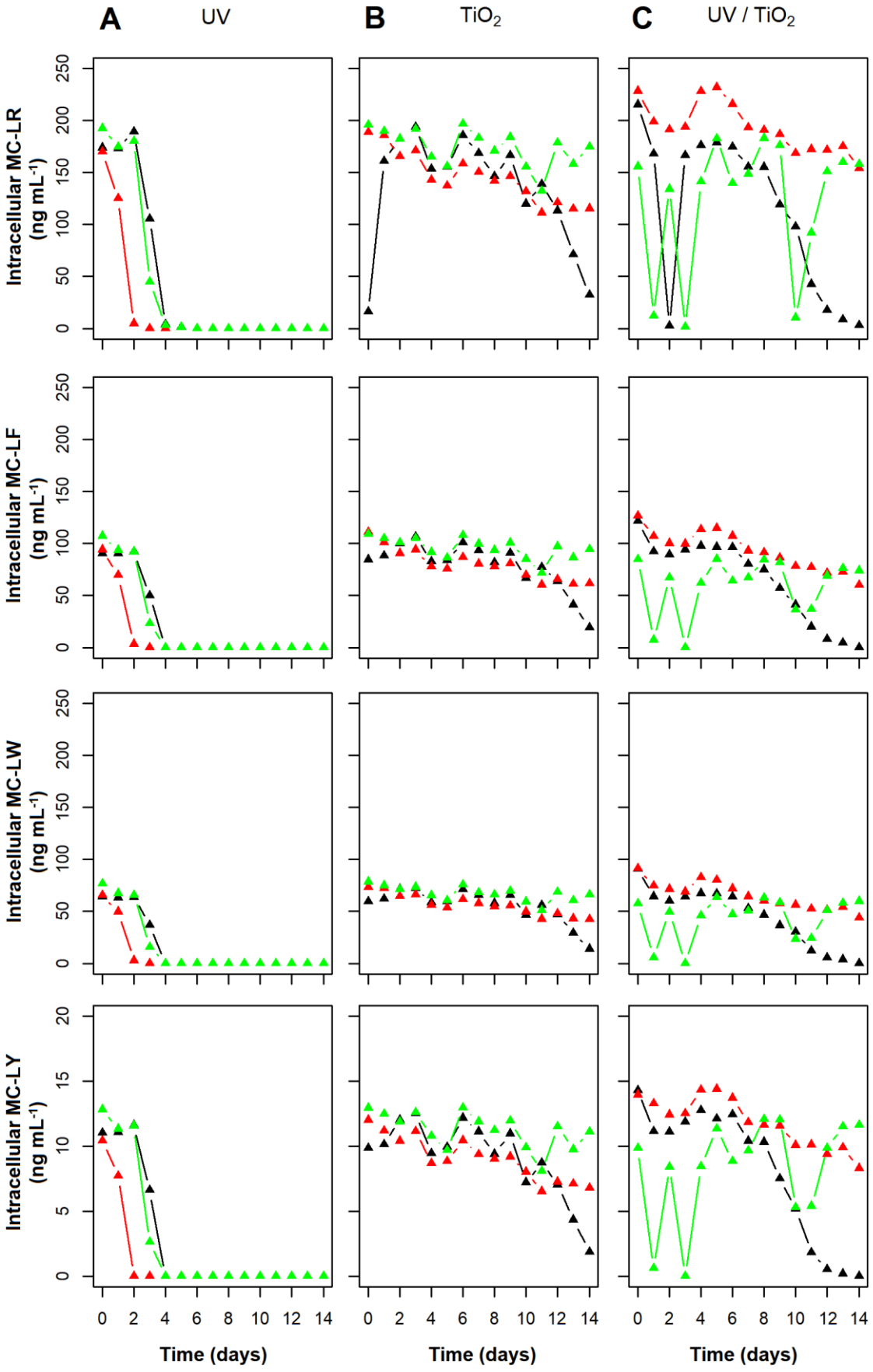
A
UV
B
TiO2
C
UV / TiO2
Intracellular MC-LR (ng mL-1)
Intracellular MC-LF (ng mL-1)
Intracellular MC-LW (ng mL-1)
Intracellular MC-LY (ng mL-1)
Time (days)

409

Figure 3 – Intracellular microcystin concentrations produced by *Microcystis aeruginosa* PCC7813 during (A) UV, (B) TiO_2 under ambient light (2.5 µmol photons m^{-2} s^{-1}) and (C) UV/TiO_2 treatment over 14 days under constant agitation. Data points represent individual replicates from each treatment.

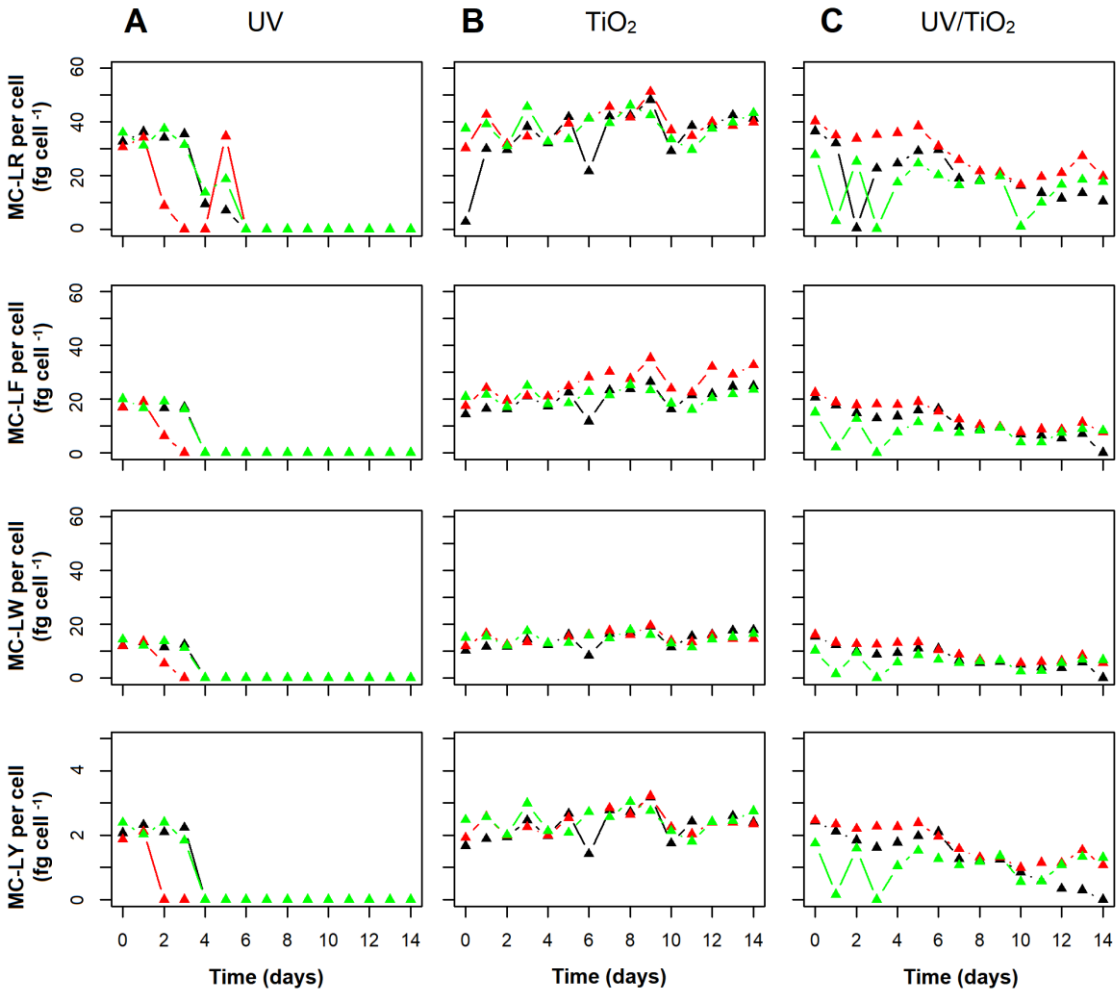

Figure 4 – Intracellular microcystin analogues ratio (toxin $cell^{-1}$) in *Microcystis aeruginosa* PCC7813 over 14 days of (A) UV, (B) TiO_2 under ambient light (2.5 µmol photons m^{-2} s^{-1}) and (C) UV/TiO_2 treatment under constant agitation. Data points represent individual replicates from each treatment.

For the UV treatment, all microcystins per cell were undetectable after 6 days (Figure 4A). The complete destruction of cells during photolysis (Figure 1A) could be confirmed by this corresponding decrease in the toxin ratio (i.e., toxin concentration per cell number). For TiO_2-only samples, the toxin concentration per cell presented variability (Figure 4B). Despite the slight decrease in cell number of TiO_2-only samples, no cell stress was detected when analyzing both photosynthetic activity (Figure 2B) and

419 intracellular toxin (Figure 3B), indicating that cells were not actually damaged and/or
420 dead but there was physical cell removal of intact healthy cells by adsorption of cells
421 onto the surface of the TiO_2 beads and the surface of the reactors.
422 The amount of toxin per cell over 14 days in the UV/TiO_2 treatment diminished by 54,
423 64, 70 and 72% for MC-LR, -LY, -LW and -LF, respectively (Figure 4C). One reason for
424 the reduction in the toxin concentration per cell could be that some of the *M.*
425 *aeruginosa* PCC7813 cells were detected and counted as living organisms, however,
426 some of the cells were probably fragmented and inactive. Additionally, as was
427 previously mentioned, intracellular microcystin could leak the cell if the cell wall was
428 compromised. Another reason for the decrease in toxin concentration could be
429 microcystins binding to intracellular proteins which *M. aeruginosa* is known to do as
430 demonstrated by Zilliges *et al*. (2011). Pestana *et al*. (2020) also observed a reduction
431 in the toxin per cell ratio of the same intracellular microcystin analogues used in the
432 present study (MC-LR, -LY, -LW and -LF) TiO_2 coated glass beads under UV/LED
433 illumination (365 nm, 2.1 mW s^{-1}), which they ascribed to microcystins binding to
434 intracellular proteins.
435 Microcystins are commonly released into the surrounding water after cell rupture by
436 water treatment processes. Therefore, water treatment technologies must be applied to
437 remove toxins that are released into the water since conventional treatment cannot
438 remove dissolved components (Chow *et al*., 1999). After the liberation of intracellular
439 microcystins during the UV treatment, samples could be best represented by a
440 piecewise regression (Figure S19 – S22) with removal for all extracellular microcystins
441 amounting to 92% for MC-LR and complete removal of the other three analogues over
442 the first 5 days (Figure 5A). The reduction in *M. aeruginosa* PCC7813 cell number
443 (Figure 1A) is the most likely reason for the decrease of intracellular microcystins
444 during the UV treatment (Figure 3A) due to cell lysis and release of the intracellular
445 content to the surrounding water followed by the immediate removal of the extracellular
446 microcystins by direct photolysis and indirect oxidation of ROS (Figure 5A). No

447 significant change (p>0.05) in the extracellular concentration of any of the microcystin
448 analogues was observed over 14 days in the TiO_2-only samples (Figure 5B), indicating
449 that there was no microcystins release from the cells. This finding also corroborates the
450 theory that cells were not destroyed in TiO_2-only samples and remained intact. During
451 UV/TiO_2 treatment, there was no increase in the extracellular microcystin
452 concentrations for most samples over 14 days (Figure 5C: red and green). However,
453 the cell reduction observed for one of the replicates (Figure 2C: black) and the decline
454 of intracellular microcystins (Figure 3C: black) of this replicate in the UV/TiO_2 treatment
455 could account for the increase of extracellular microcystins (Figure 5C: black). The
456 toxin concentration released in this replicate (Figure 5C: black) corresponds to the
457 concentration increase of the extracellular microcystins, an indication of cell lysis
458 caused by the UV/TiO_2.
459

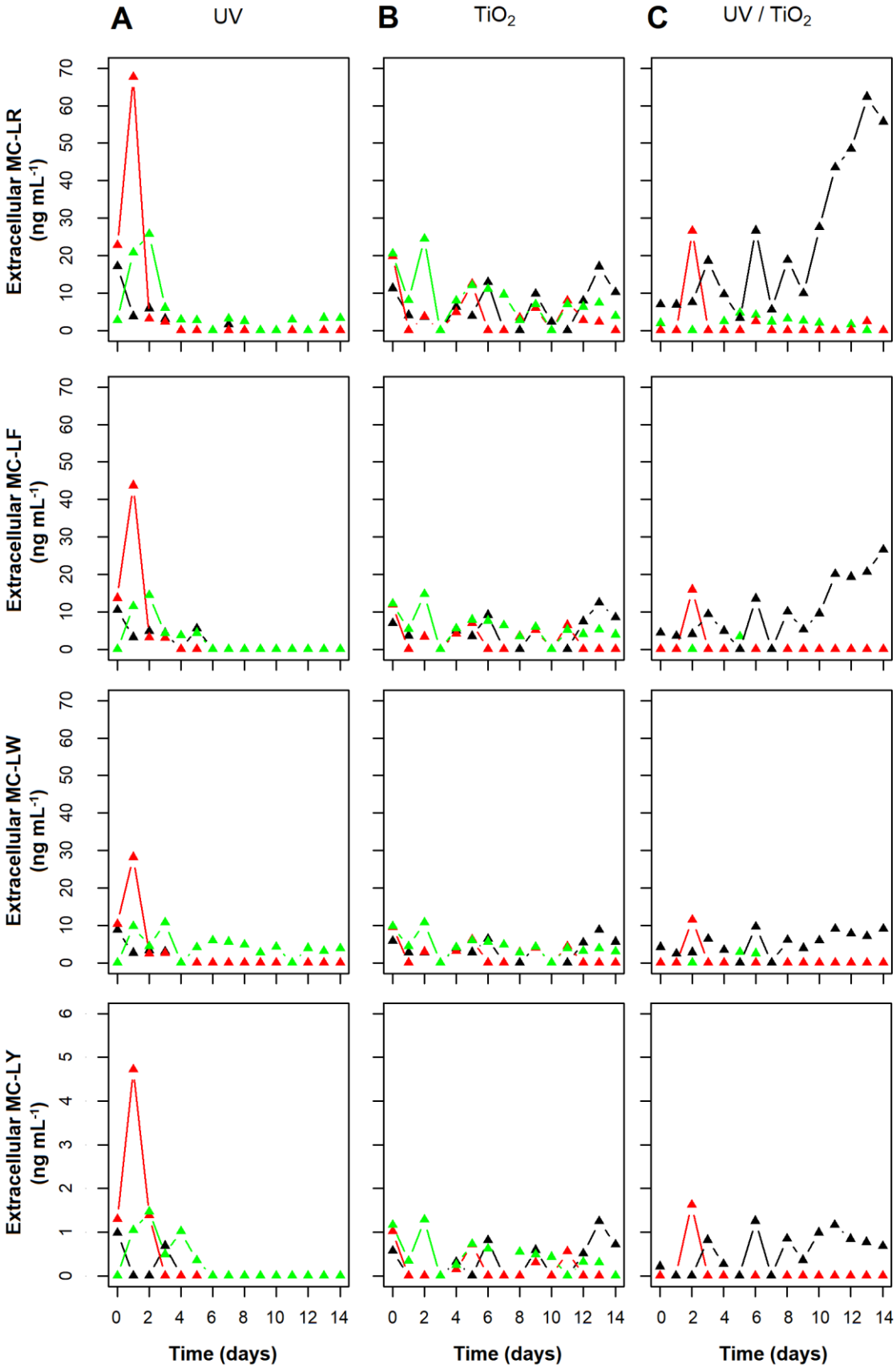

460

Figure 5 – Extracellular microcystin analogue concentrations produced by *Microcystis*

aeruginosa PCC7813 during (A) UV, (B) TiO_2 under ambient light (2.5 µmol photons m^{-2} s^{-1}) and (C) UV/TiO_2 treatment over 14 days under constant agitation. Data points represent individual replicates from each treatment.

461

462 A study by Robertson *et al*. (1999) evaluated the destruction of MC-LR under UV/TiO_2
463 photocatalysis and photolysis in the presence of phycocyanin. The authors also
464 observed a decline of MC-LR concentration when the sample was treated with only UV-
465 A light in the presence of phycocyanin, corroborating the results of the current study.
466 However, when no phycocyanin was present, the UV light had no effect on the toxin
467 degradation, showing that phycocyanin acts as a photocatalyst for microcystin
468 destruction under UV illumination until the pigment was completely bleached
469 (Robertson *et al*., 1999). There is a number of studies which have investigated the
470 effects of UV illumination on microcystins (Liu *et al*., 2010; Pinho *et al*., 2015a, 2015b,
471 2012; Triantis *et al*., 2012), however, the breakdown of pure microcystin requires UV-C.
472 In order for the UV-A illumination used in the current study to breakdown microcystins,
473 the presence of phycocyanin is necessary. Similar effects were observed by Rinalducci
474 *et al.* (2008) which demonstrated the photosensitizing effect of phycocyanin on the
475 phycobilisomes of another cyanobacterium (Synechocystis PCC 6803).
476 Pestana *et al*. (2020) carried out a bench-scale (30 mL of cell suspension) study of the
477 destruction *M. aeruginosa* strain (PCC7813) (MC-LR, -LY, -LF and -LW) under UV/TiO_2
478 photocatalysis the TiO_2 coated beads used in the current study. Intracellular microcystin
479 analogues were removed by 49% and extracellular microcystins that were release after
480 cell lysis were completely removed by UV/TiO_2 photocatalysis. Similar results were
481 expected in the current study, however, UV photolysis was more efficient for the
482 removal of microcystins than the UV/TiO_2 photocatalytic treatment used in the present
483 study. The difference in the results might have occurred due to the larger scale and
484 lower initial cell concentration (6.5 L with 5 x 10^6 cells mL^{-1} in the current study
485 compared to 30 mL with 15 x 10^6 cells mL^{-1} used in Pestana *et al*. (2020) study).
486 Further, in the current study, a small amount of cell growth was observed in UV/TiO_2

487 treatment over the first 8 days (Figure 1C). Additionally, stronger mixing caused by the
488 multi-porous air-stone in the base of the reactor in the current study combined with the
489 dispersion of the larger air bubbles by the TiO_2-coated glass beads that potentially
490 attenuated the effects of the UV irradiation, rendering the UV/TiO_2 treatment less
491 effective. In contrast, in the Pestana *et al*. (2020) study, only very gentle single point
492 sparging (flow rate of 1.5 L min^{-1}) was used from the top of the vials. Finally, the
493 shadowing effect caused by the coated glass beads and the stainless-steel pods inside
494 the reactors (which were not used in the Pestana *et al*. (2020) study) may have
495 interfered in the efficiency of the photocatalytic removal of the microcystins.
496
497 **3.3 *Microcystis aeruginosa* PCC7813 regrowth post UV and UV/TiO_2 treatment**
498 It is important to evaluate cyanobacterial regrowth potential to determine the residual
499 effects of the treatment. For the UV-A treated cells the difference in cell concentration
500 between the beginning of the regrowth experiment and day 6 was not significant
501 (p=0.08) due to the fact that few cells remained viable after UV treatment that were not
502 inhibited/damaged (Figure 6A). The remaining *M. aeruginosa* PCC7813 cells had a
503 doubling rate of 1.9 days over 6 days of regrowth (Figure 6A), which is still considered
504 a typical doubling rate for *M. aeruginosa*. For the TiO_2-only samples, variability was
505 high, with one of the replicates (Figure 6B: black) which had the lowest cell density
506 after 14 days treatment with TiO_2-only showing no regrowth. This replicate (Figure 6B:
507 black) actually showed a decreased in cell density from 4.1 x 10^5 to 2.5 x 10^5 cells mL^{-1}
508 over 6 days, while the other two replicates (Figure 6B: red and green) presented a
509 doubling rate of 2.9 and 3.8 days, respectively. The same sample variability was
510 observed in regrowth samples from the UV/TiO_2 treatment (Figure 6C). While cell
511 concentrations in two replicates (Figure 6C: black and green) doubled at a rate of 4.2
512 and 4.7 days respectively, the third replicates (Figure 6C: red) decreased in cell density
513 from 4.1 x 10^6 to 1.4 x 10^5 cells mL^{-1} over 6 days.
514 Wilson *et al*. (2006) stated an average doubling rate for 32 strains of *Microcystis*

515 cultured in BG-11 medium as 2.8 days. Some UV treatment samples from the current
516 study presented a faster doubling rate of 1.9 days and some UV/TiO_2 treatment
517 samples showed a slower doubling rate of 4.2 and 4.7 days.
518 Despite the lower initial cell density after 6 days of regrowth in UV treatment (Figure
519 6A), the cells in UV treatment showed the fastest doubling rate (1.9 days) when
520 compared to cells from TiO_2-only samples and UV/TiO_2 treatment (Figures 6B and C),
521 as previously observed by Dunn and Manoylov (2016). In the UV treatment, low cell
522 density means low competition for resources, hence this is often when growth is
523 fastest.
524

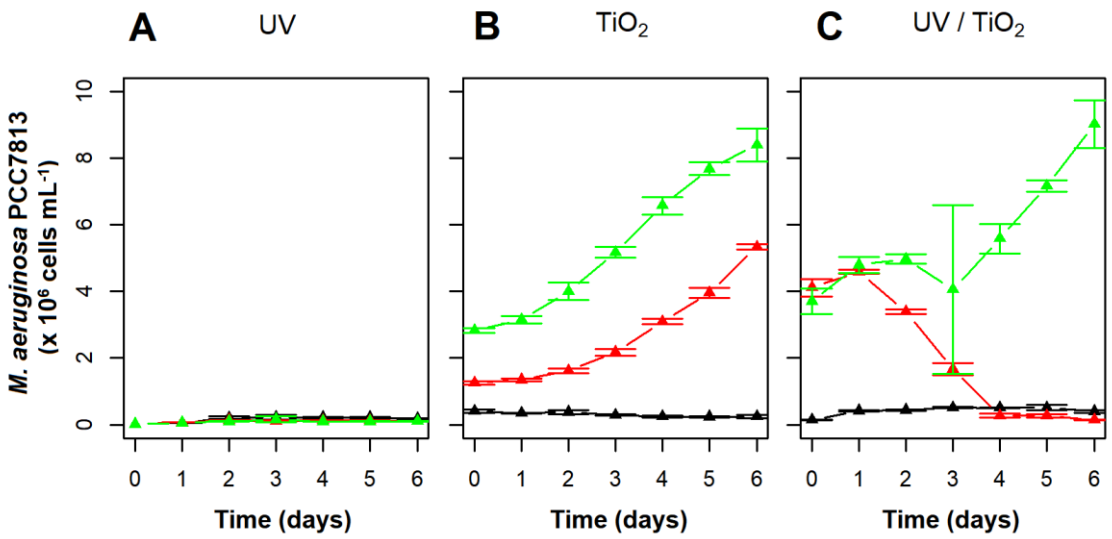

Figure 6 – Effects of (A) UV-LED irradiation (365 nm), (B) TiO_2 coated glass beads under ambient light (2.5 µmol photons m^{-2} s^{-1}) and (C) photocatalytic treatment on *Microcystis aeruginosa* PCC7813 regrowth using TiO_2 coated glass beads under UV-LED illumination (365 nm) over seven days under cool white fluorescent lights of 10.5 µmol photons m^{-2} s^{-1}. Data points represent the average of four replicates from each treatment where four individual vials were used for samples of each tested system (UV-only, TiO_2-only and UV/TiO_2) to assess regrowth (*n* = 4).

Ou *et al*. (2012) studied the effects of different UV-C dosages (140-4200 mJ cm^{-2}) on *M. aeruginosa* FACHB-912 recovery over 7 days. They found a significant reduction in indicators of photosynthesis (e.g., quantum yield) and chlorophyll a for samples irradiated at 350, 700, 1400 and 4200 mJ cm^{-2}, showing the irreversible inhibition of the photosynthetic system in the *M. aeruginosa* cells FACHB-912 after UV-C irradiation which then inhibited the reproduction and recovery of *M. aeruginosa* cells (Ou *et al*., 2012).

A study by Huang *et al*. (2011) evaluated the regrowth potential of *M. aeruginosa* after 24 hours of ZnO/γ-Al_2O_3 photocatalytic treatment under solar light. After 12 days of regrowth, the cell density of treated samples was less than 85% of that of the control, highlighting the lasting effect of photocatalysis on *M. aeruginosa* cells even though a

538 different type of photocatalyst and irradiation was applied (Huang *et al.*, 2011).

539

540 **4 Conclusion**

541 The current study investigated the effects of UV-A photolysis and a UV/TiO_2
542 photocatalytic system using TiO_2 coated glass beads on *M. aeruginosa* PCC7813 cells
543 and the four main microcystin analogues (MC-LR, -LY, -LW and -LF) this strain
544 produces. Both systems had energy-efficient UV illumination supplied by UV-LEDs for
545 cyanobacteria and cyanotoxin control. The UV photolysis was able to consistently
546 remove cyanobacterial cells and toxins, and therefore was shown to be more effective
547 than the UV/TiO_2 photocatalytic system which gave a delayed removal of cells and
548 concerningly, slightly supported growth in the first 8 days. All the data analysis (cell
549 density, photosynthetic activity, toxin per cell, intra- and extracellular toxin) indicate that
550 UV-A photolysis was capable of not only inhibiting *M. aeruginosa* PCC7813 cells, but it
551 significantly damaged them to the point that only a very limited regrowth was observed.
552 An advantage of using UV-A irradiation over other types of UV irradiation is that UV-A
553 illumination might be specific to cyanobacterial control due to the presence of
554 phycocyanin inside of the cyanobacterial cells. To confirm this, the effects of UV
555 photolysis on other phytoplankton (diatoms and green algae) and cyanobacterial
556 species shouldbe investigated, such as a mesocosms experiment with community
557 analysis. An additional advantage of employing UV-A over other types of UV irradiation
558 is that lamps generating UV-A tend to be more economical in terms of capital cost
559 compared to UV-B or UV-C generating lamps. In practice, many aspects of the reactor
560 design need to be optimized and field-tested to allow *in-situ* application inside
561 reservoirs: vertical or horizontal orientation of reactors, optimization of the active
562 surface area and contact time, incorporation of waterproof UV-LEDs, and powering the
563 units *in-situ* exploring solar options. The current study has successfully demonstrated
564 that UV-LED-based advanced oxidation techniques could be operated at a larger-than-

565 bench scale and control cyanobacteria and their toxins.

566

567 **5 Acknowledgements**

568 The authors would like to thank the Engineering and Physical Sciences Research
569 Council (EPSRC) [EP/P029280/1], the Coordination for the Improvement of
570 Higher Education Personnel - CAPES [PROEX 20/2016 and PrInt
571 88887.311806/2018-00], and the Brazilian National Research Council – CNPq
572 [403116/2016-3 and 304164/2017-8] for funding this research. As per EPSRC
573 requirement all data will be made publicly available via the Robert Gordon
574 University's open access repository OpenAIR@RGU. Further, the first author also
575 acknowledges the scholarship from the Brazilian National Research Council -
576 CNPq. Finally, Len Montgomery is appreciated for proof-reading the manuscript
577 and the authors would like to thank Dr Nathan Skillen of Queen's University
578 Belfast, for help and guidance with the electrical wiring of the LEDS for the
579 reactors.

580

581 **6 References**

582 Akkanen, J., Kukkonen, J.V.K., 2003. Measuring the bioavailability of two hydrophobic
583 organic compounds in the presence of dissolved organic matter. Environ. Toxicol.
584 Chem. 22, 518–524.

585 Boyd, B., Suslov, S.A., Becker, S., Greentree, A.D., Maksymov, I.S., 2020. Beamed UV
586 sonoluminescence by aspherical air bubble collapse near liquid-metal
587 microparticles. Sci. Rep. 10, 1–8. https://doi.org/10.1038/s41598-020-58185-2

588 Carmichael, W.W., Azevedo, S.M.F.O., An, J.S., Molica, R.J.R., Jochimsen, E.M., Lau,
589 S., Rinehart, K.L., Shaw, G.R., Eaglesham, G.K., 2001. Human fatalities form
590 cyanobacteria: Chemical and biological evidence for cyanotoxins. Environ. Health
591 Perspect. 109, 663–668. https://doi.org/10.1289/ehp.01109663

592 Chae, S., Noeiaghaei, T., Oh, Y., Kim, I.S., Park, J.S., 2019. Effective removal of
593 emerging dissolved cyanotoxins from water using hybrid photocatalytic composites.
594 Water Res. 149, 421–431. https://doi.org/10.1016/j.watres.2018.11.016

595 Chang, C.W., Huo, X., Lin, T.F., 2018. Exposure of *Microcystis aeruginosa* to hydrogen
596 peroxide and titanium dioxide under visible light conditions: Modeling the impact of
597 hydrogen peroxide and hydroxyl radical on cell rupture and microcystin degradation.
598 Water Res. 141, 217–226. https://doi.org/10.1016/j.watres.2018.05.023

599 Chen, L., Zhao, C., Dionysiou, D.D., O'Shea, K.E., 2015. TiO_2 photocatalytic degradation
600 and detoxification of cylindrospermopsin. J. Photochem. Photobiol. A Chem. 307–
601 308, 115–122. https://doi.org/10.1016/j.jphotochem.2015.03.013

602 Chow, C.W.K., Drikas, M., House, J., Burch, M.D., Velzeboer, R.M.A., 1999. The impact
603 of conventional water treatment processes on cells of the cyanobacterium
604 *Microcystis aeruginosa*. Water Res. 33, 3253–3262. https://doi.org/10.1016/S0043-
605 1354(99)00051-2

606 Drábková, Michaela, Admiraal, W., Maršálek, B., 2007a. Combined exposure to
607 hydrogen peroxide and light-selective effects on cyanobacteria, green algae, and
608 diatoms. Environ. Sci. Technol. 41, 309–314. https://doi.org/10.1021/es060746i

609 Drábková, M., Matthijs, H.C.P., Admiraal, W., Maršálek, B., 2007b. Selective effects of
610 H_2O_2 on cyanobacterial photosynthesis. Photosynthetica 45, 363–369.
611 https://doi.org/10.1007/s11099-007-0062-9

612 Dunn, R.M., Manoylov, K.M., 2016. The Effects of Initial Cell Density on the Growth and
613 Proliferation of the Potentially Toxic Cyanobacterium *Microcystis aeruginosa* J.
614 Environ. Prot. (Irvine,. Calif). 07, 1210–1220.
615 https://doi.org/10.4236/jep.2016.79108

616 Falconer, I.R., Beresford, A.M., Runnegar, M.T.C., 1983. Evidence of liver damage by
617 toxin from a bloom of the blue-green alga, *Microcystis aeruginosa*. Med. J. Aust. 1,
618 511–514. https://doi.org/10.5694/j.1326-5377.1983.tb136192.x

619 Fan, F., Shi, X., Zhang, M., Liu, C., Chen, K., 2019. Comparison of algal harvest and
620 hydrogen peroxide treatment in mitigating cyanobacterial blooms via an *in situ*
621 mesocosm experiment. Sci. Total Environ. 694, 133721.
622 https://doi.org/10.1016/j.scitotenv.2019.133721

623 Heering, W., 2004. UV-sources - Basics, Properties and Applications. Int. Ultrav. Assoc.
624 6, 7–13.

625 Hu, Xi, Hu, Xinjiang, Tang, C., Wen, S., Wu, X., Long, J., Yang, X., Wang, H., Zhou, L.,
626 2017. Mechanisms underlying degradation pathways of microcystin-LR with doped
627 TiO_2 photocatalysis. Chem. Eng. J. 330, 355–371.
628 https://doi.org/10.1016/j.cej.2017.07.161

629 Huang, W.J., Lin, T.P., Chen, J.S., Shih, F.H., 2011. Photocatalytic inactivation of
630 cyanobacteria with ZnO/γ-Al_2O_3 composite under solar light. J. Environ. Biol. 32,
631 301–307.

632 Hui, J., Pestana, C.J., Caux, M., Gunaratne, H.Q.N., Edwards, C., Robertson, P.K.J.,
633 Lawton, L.A., Irvine, J.T.S., 2021. Graphitic-C_3N_4 coated floating glass beads for
634 photocatalytic destruction of synthetic and natural organic compounds in water
635 under UV light. J. Photochem. Photobiol. A Chem. 405, 112935.
636 https://doi.org/10.1016/j.jphotochem.2020.112935

637 Jin, Y., Zhang, S., Xu, H., Ma, C., Sun, J., Li, H., 2019. Application of N-TiO_2 for visible-
638 light photocatalytic degradation of *Cylindrospermopsis raciborskii*. More difficult
639 than that for photodegradation of *Microcystis aeruginosa*?. Environ. Pollut. 245,
640 642–650. https://doi.org/10.1016/j.envpol.2018.11.056

641 Jochimsen, E.., Carmichael, W.W., An, J., Cardo, D.M., Cookson, S.T.; Holmes, C.E.M.;
642 Antunes, B.C.; Melo Filho, D.A.; Lyra, T.M.; Barreto, V.S.T; Azevedo, S.M.F.O. &
643 Jarvis, W.., 1998. Liver failure and death after exposure to microcystins. N. Engl. J.
644 Med. 338, 873–878. https://doi.org/10.1080/13504509.2013.856048 M4 - Citavi

645 Li, L., Sahi, S.K., Peng, M., Lee, E.B., Ma, L., Wojtowicz, J.L., Malin, J.H., Chen, W.,
646 2016. Luminescence-and nanoparticle-mediated increase of light absorption by
647 photoreceptor cells: Converting UV light to visible light. Sci. Rep. 6.
648 https://doi.org/10.1038/srep20821

649 Liu, X., Chen, Z., Zhou, N., Shen, J., Ye, M., 2010. Degradation and detoxification of
650 microcystin-LR in drinking water by sequential use of UV and ozone. J. Environ. Sci.
651 22, 1897–1902. https://doi.org/10.1016/S1001-0742(09)60336-3

652 Mathew, S., Kumar Prasad, A., Benoy, T., Rakesh, P.P., Hari, M., Libish, T.M.,
653 Radhakrishnan, P., Nampoori, V.P.N., Vallabhan, C.P.G., 2012. UV-visible
654 photoluminescence of TiO_2 nanoparticles prepared by hydrothermal method. J.
655 Fluoresc. 22, 1563–1569. https://doi.org/10.1007/s10895-012-1096-3

656 Matthijs, H.C.P., Visser, P.M., Reeze, B., Meeuse, J., Slot, P.C., Wijn, G., Talens, R.,
657 Huisman, J., 2012. Selective suppression of harmful cyanobacteria in an entire lake
658 with hydrogen peroxide. Water Res. 46, 1460–1472.
659 https://doi.org/10.1016/j.watres.2011.11.016

660 Menezes, I., Maxwell-mcqueeney, D., Pestana, C.J., Edwards, C., Lawton, L.A., 2020.
661 Oxidative stress in the cyanobacterium *Microcystis aeruginosa* PCC 7813 :
662 Comparison of different analytical cell stress detection assays. Chemosphere 269

128766. https://doi.org/10.1016/j.chemosphere.2020.128766

Moon, B.R., Kim, T.K., Kim, M.K., Choi, J., Zoh, K.D., 2017. Degradation mechanisms of Microcystin-LR during UV-B photolysis and UV/H_2O_2 processes: Byproducts and pathways. Chemosphere 185, 1039–1047. https://doi.org/10.1016/j.chemosphere.2017.07.104

Ou, H., Gao, N., Deng, Y., Qiao, J., Wang, H., 2012. Immediate and long-term impacts of UV-C irradiation on photosynthetic capacity, survival and microcystin-LR release risk of *Microcystis aeruginosa*. Water Res. 46, 1241–1250. https://doi.org/10.1016/j.watres.2011.12.025

Ou, H., Gao, N., Deng, Y., Qiao, J., Zhang, K., Li, T., Dong, L., 2011a. Mechanistic studies of *Microcystic aeruginosa* inactivation and degradation by UV-C irradiation and chlorination with poly-synchronous analyses. DES 272, 107–119. https://doi.org/10.1016/j.desal.2011.01.014

Ou, H., Gao, N., Deng, Y., Wang, H., Zhang, H., 2011b. Inactivation and degradation of *Microcystis aeruginosa* by UV-C irradiation. Chemosphere 85, 1192–1198. https://doi.org/10.1016/j.chemosphere.2011.07.062

Pattanaik, B., Schumann, R., Karsten, U., 2007. Effects of Ultraviolet Radiation on Cyanobacteria and Their Protective Mechanisms. Limnology 29–45.

Pestana, C.J., Capelo-Neto, J., Lawton, L., Oliveira, S., Carloto, I., Linhares, H.P., 2019. The effect of water treatment unit processes on cyanobacterial trichome integrity. Sci. Total Environ. 659, 1403–1414. https://doi.org/10.1016/j.scitotenv.2018.12.337

Pestana, C.J., Portela Noronha, J., Hui, J., Edwards, C., Gunaratne, H.Q.N., Irvine, J.T.S., Robertson, P.K.J., Capelo-Neto, J., Lawton, L.A., 2020. Photocatalytic removal of the cyanobacterium *Microcystis aeruginosa* PCC7813 and four microcystins by TiO_2 coated porous glass beads with UV-LED irradiation. Sci. Total Environ. 745, 141154. https://doi.org/10.1016/j.scitotenv.2020.141154

Pinho, L.X., Azevedo, J., Brito, A., Santos, A., Tamagnini, P., Vilar, V.J.P., Vasconcelos, V.M., Boaventura, R.A.R., 2015a. Effect of TiO_2 photocatalysis on the destruction of *Microcystis aeruginosa* cells and degradation of cyanotoxins microcystin-LR and cylindrospermopsin. Chem. Eng. J. 268, 144–152. https://doi.org/10.1016/j.cej.2014.12.111

Pinho, L.X., Azevedo, J., Miranda, S.M., Ângelo, J., Mendes, A., Vilar, V.J.P., Vasconcelos, V., Boaventura, R.A.R., 2015b. Oxidation of microcystin-LR and cylindrospermopsin by heterogeneous photocatalysis using a tubular photoreactor

packed with different TiO_2 coated supports. Chem. Eng. J. 266, 100–111. https://doi.org/10.1016/j.cej.2014.12.023

Pinho, L.X., Azevedo, J., Vasconcelos, V.M., Vilar, V.J.P., Boaventura, R.A.R., 2012. Decomposition of *Microcystis aeruginosa* and microcystin-LR by TiO_2 oxidation using artificial UV light or natural sunlight. J. Adv. Oxid. Technol. 15, 98–106. https://doi.org/10.1515/jaots-2012-0111

Rinalducci, S., Pedersen, J.Z., Zolla, L., 2008. Generation of reactive oxygen species upon strong visible light irradiation of isolated phycobilisomes from *Synechocystis* PCC 6803. Biochim. Biophys. Acta - Bioenerg. 1777, 417–424. https://doi.org/10.1016/j.bbabio.2008.02.005

Robertson, P.K.J., Lawton, L.A., Cornish, B.J.P.A., 1999. The Involvement of Phycocyanin Pigment in the Photodecomposition of the Cyanobacterial Toxin, Microcystin-LR. J. Porphyr. Phthalocyanines 3, 544–551. https://doi.org/10.1002/(sici)1099-1409(199908/10)3:6/7<544::aid-jpp173>3.0.co;2-7

Sinha, A.K., Eggleton, M.A., Lochmann, R.T., 2018. An environmentally friendly approach for mitigating cyanobacterial bloom and their toxins in hypereutrophic ponds: Potentiality of a newly developed granular hydrogen peroxide-based compound. Sci. Total Environ. 637–638, 524–537. https://doi.org/10.1016/j.scitotenv.2018.05.023

Song, J., Wang, Xuejiang, Ma, J., Wang, Xin, Wang, J., Xia, S., Zhao, J., 2018. Removal of *Microcystis aeruginosa* and Microcystin-LR using a graphitic-C_3N_4/TiO_2 floating photocatalyst under visible light irradiation. Chem. Eng. J. 348, 380–388. https://doi.org/10.1016/j.cej.2018.04.182

Spoof, L., Catherine, A., 2017. Cyanobacteria samples: preservation, abundance and biovolume measurements, in: Meriluoto, J., Spoof, L., A. Codd, G. (Eds.), Handbook of Cyanobacterial Monitoring and Cyanotoxin Analysis. John Wiley & Sons, Chichester, UK, pp. 526–537. https://doi.org/10.1002/9781119068761

Stanier, R.Y., Kunisawa, R., Mandel, M., Cohen-Bazire, G., 1971. Purification and properties of unicellular blue-green algae (order *Chroococcales*). Bacteriol. Rev. 35, 171–205. https://doi.org/10.1128/mmbr.35.2.171-205.1971

Stirbet, A., Lazár, D., Papageorgiou, G.C., Govindjee, 2018. Chlorophyll *a* Fluorescence in Cyanobacteria: Relation to Photosynthesis, Cyanobacteria: From Basic Science to Applications. https://doi.org/10.1016/B978-0-12-814667-5.00005-2

731 Summerfelt, S.T., 2003. Ozonation and UV irradiation - An introduction and examples of
732 current applications. Aquac. Eng. 28, 21–36. https://doi.org/10.1016/S0144-
733 8609(02)00069-9

734 Tao, Y., Hou, D., Zhou, T., Cao, H., Zhang, W., Wang, X., 2018. UV-C suppression on
735 hazardous metabolites in *Microcystis aeruginosa*: Unsynchronized production of
736 microcystins and odorous compounds at population and single-cell level. J. Hazard.
737 Mater. 359, 281–289. https://doi.org/10.1016/j.jhazmat.2018.07.052

738 Triantis, T.M., Fotiou, T., Kaloudis, T., Kontos, A.G., Falaras, P., Dionysiou, D.D., Pelaez,
739 M., Hiskia, A., 2012. Photocatalytic degradation and mineralization of microcystin-
740 LR under UV-A, solar and visible light using nanostructured nitrogen doped TiO_2. J.
741 Hazard. Mater. 211–212, 196–202. https://doi.org/10.1016/j.jhazmat.2011.11.042

742 Vilela, W.F.D., Minillo, A., Rocha, O., Vieira, E.M., Azevedo, E.B., 2012. Degradation of
743 [D-Leu]-Microcystin-LR by solar heterogeneous photocatalysis (TiO_2). Sol. Energy
744 86, 2746–2752. https://doi.org/10.1016/j.solener.2012.06.012

745 Wang, Xin, Wang, Xuejiang, Zhao, J., Song, J., Su, C., Wang, Z., 2018. Surface modified
746 TiO_2 floating photocatalyst with PDDA for efficient adsorption and photocatalytic
747 inactivation of *Microcystis aeruginosa*. Water Res. 131, 320–333.
748 https://doi.org/10.1016/j.watres.2017.12.062

749 Wang, Xin, Wang, Xuejiang, Zhao, J., Song, J., Wang, J., Ma, R., Ma, J., 2017. Solar
750 light-driven photocatalytic destruction of cyanobacteria by F-Ce-TiO_2/expanded
751 perlite floating composites. Chem. Eng. J. 320, 253–263.
752 https://doi.org/10.1016/j.cej.2017.03.062

753 Wilson, A.E., Wilson, W.A., Hay, M.E., 2006. Intraspecific variation in growth and
754 morphology of the bloom-forming cyanobacterium *Microcystis aeruginosa*. Appl.
755 Environ. Microbiol. 72, 7386–7389. https://doi.org/10.1128/AEM.00834-06

756 Yang, W., Tang, Z., Zhou, F., Zhang, W., Song, L., 2013. Toxicity studies of tetracycline
757 on *Microcystis aeruginosa* and *Selenastrum capricornutum*. Environ. Toxicol.
758 Pharmacol. 35, 320–324. https://doi.org/10.1016/j.etap.2013.01.006

759 Yang, Z., Kong, F., Shi, X., Yu, Y., Zhang, M., 2015. Effects of UV-B radiation on
760 microcystin production of a toxic strain of *Microcystis aeruginosa* and its
761 competitiveness against a non-toxic strain. J. Hazard. Mater. 283, 447–453.
762 https://doi.org/10.1016/j.jhazmat.2014.09.053

763 Zhao, C., Pelaez, M., Dionysiou, D.D., Pillai, S.C., Byrne, J.A., O'Shea, K.E., 2014. UV
764 and visible light activated TiO_2 photocatalysis of 6-hydroxymethyl uracil, a model

765 compound for the potent cyanotoxin cylindrospermopsin. Catal. Today 224, 70–76.
766 https://doi.org/10.1016/j.cattod.2013.09.042

767 Zilliges, Y., Kehr, J.C., Meissner, S., Ishida, K., Mikkat, S., Hagemann, M., Kaplan, A.,
768 Börner, T., Dittmann, E., 2011. The cyanobacterial hepatotoxin microcystin binds to
769 proteins and increases the fitness of *Microcystis* under oxidative stress conditions.
770 PLoS One 6. https://doi.org/10.1371/journal.pone.0017615

771